NATIONAL ADVISORY COMMITTEE FOR AERONAUTICS

SPECIAL REPORT No. 133

PRESSURE DISTRIBUTION ON THE FUSELAGE OF A MIDWING AIRPLANE MODEL AT HIGH SPEEDS

By James B. Delano
Langley Memorial Aeronautical Laboratory

November 1939

PRESSURE DISTRIBUTION ON THE FUSELAGE OF A MIDWING AIRPLANE MODEL AT HIGH SPEEDS

By James B. Delano

SUMMARY

The pressure distribution on the fuselage of a midwing airplane model was measured in the N.A.C.A. 8-foot high-speed wind tunnel at speeds from 140 to 440 miles per hour for lift coefficients ranging from -0.2 to 1.0. The primary purpose of the tests was to provide data showing the air pressures on various parts of the fuselage for use in structural design. The data may also be used for the design of scoops and vents.

The results show that the highest negative pressures occurred near the wing and were more dependent on the wing than on the fuselage. At high speeds, the magnitude of the pressure coefficients as predicted from pressure coefficients determined experimentally at low speeds by application of the theoretical factor $1/\sqrt{1-M^2}$ (where M is the ratio of the air speed to the speed of sound in air) may misrepresent the actual conditions. At the points where the maximum negative pressures occurred, however, the variation of the pressure coefficients was in good agreement with the theoretical factor, indicating that this factor may afford satisfactory predictions of critical speed, at least for fuselages similar to the shape tested.

INTRODUCTION

The local pressures on some parts of the fuselages of high-speed airplanes are so large that they must be considered in the structural design, especially of such parts as doors over bomb bays and other openings. The primary purpose of the present investigation was to provide data useful in the structural design of such parts. The data are also useful for the design of air scoops and vents (reference 1).

The tests were made in the N.A.C.A. 8-foot high-speed wind tunnel (reference 2) with a model wing mounted on a model fuselage without propeller or tail surfaces. The test speeds were extended up to 440 miles per hour to ascertain the effects of compressibility on the pressures. The fuselage angles of attack ranged from -3° to 9° corresponding to lift coefficients from -0.2 to 1.0. The Reynolds Number range, based on the mean chord of the model (17.29 inches), was 1,700,000 to 4,800,000.

APPARATUS AND METHOD

The fuselage was a body of revolution of N.A.C.A. form 111 (reference 3) modified to a fineness ratio of 6.06. The wing (fig. 1) was a 1/8-scale model of the DC-3 transport wing, which has a root section of N.A.C.A. 2215 profile, and was set at an incidence of -1° to the fuselage axis. The wing tips extended through the tunnel wall to support the model. Tail surfaces and propeller were omitted. Thirty-nine pressure orifices located as shown in figure 2 were used. The pressure tubes were led out of the tail end of the fuselage (fig. 1(b)) and connected to a multiple-tube manometer where all the pressures were photographically recorded at one time. This investigation was made in the N.A.C.A. 8-foot high-speed wind tunnel, a single-return, closed-throat wind tunnel of circular cross section.

RESULTS

The results have been corrected for constriction effects and are presented as nondimensional pressure coefficients:

$$P = \frac{\Delta p}{q}$$

where Δp is the local static pressure on the fuselage less the static pressure of the air stream.

q, dynamic pressure of the air stream $(1/2\ \rho V^2)$.

The Mach number M is the ratio of the air speed to the speed of sound in air at the temperature of the tests.

In all the figures showing values of P for fuselage angles of attack $\alpha_f = 0^\circ$ and 6°, the values for speeds below 200 miles per hour (M = 0.265) were taken from cross plots against α_f; consequently, experimental points are not shown. The location of a point along any meridian of the fuselage is given by x/L, where x is the distance along the axis of the fuselage measured from the nose and L is the length of the fuselage. Figure 3 is a plot of the lift coefficient for M = 0.182 (140 miles per hour at 59° F.) for the fuselage angles of attack used in these tests. Figures 4 to 8 present the pressure distributions along various meridians of the fuselage as plots of P, with the meridian angle ω (fig. 2) and the fuselage angle of attack as parameters, for M = 0.182. A comparison is shown in figure 9 between experimental pressures obtained on the wing-fuselage combination and the theoretical pressures on the fuselage alone and on the wing alone for $\alpha_f = 0^\circ$. Figures 10 and 11 show plots of P along the top and the bottom meridians ($\omega = 0^\circ$ and 180°), respectively, with α_f as a parameter, for M = 0.182.

The variation of P with M at the different meridian angles is shown in figures 12 to 16 for $\alpha_f = 0^\circ$. At high speeds, the scatter of the experimental points increases. This increase is due mainly to the use of mercury to measure the pressures at high speeds; whereas alcohol and carbon tetrachloride were used at lower speeds. The results for $\alpha_f = -1^\circ$ were essentially the same as those for $\alpha_f = 0^\circ$ and are therefore not presented herein. Comparisons between the experimental variation with speed of the maximum negative pressure coefficients and the theoretical variation given by $P_o/\sqrt{1-M^2}$, where P_o is the value of P at M = 0, are given in figure 17.

DISCUSSION

Figures 4 to 9 show, as would be expected, that the higher negative pressures on the fuselage surface occurred near portions of the wing which produced the highest negative pressures. At low speeds, the presence of the wing increased the maximum negative pressure coefficient on the fuselage from P = -0.140 to -0.340. (See fig. 9.) At 400 miles per hour, the load increased by 0.24q, which, at standard sea-level conditions, represents approximately 100 pounds per square foot. It is believed that the in-

crease in air loads will be higher for points closer to the wing than for those used in these tests.

Figure 10 shows that the maximum negative pressure coefficient along the top of the fuselage ($\omega = 0^\circ$) is almost directly proportional to α_f; whereas figures 4 to 9 show that, along the 45° meridian, the rate of change of the maximum negative pressure coefficient is greater and increases more rapidly as α_f is increased, at least for the angles of attack used in these tests. The pressures over the fuselage alone were not measured, but an analysis of the pressures over an airship hull reported in reference 4 shows that the magnitude of the maximum negative pressures on the fuselage at large angles of attack will still be largely dependent on the wing. Figures 5 and 8 show that an increase in α_f from 0° to 9° may triple the value of P. The maximum structural loads, nevertheless, will generally occur at high speeds.

For two-dimensional flow, a theoretical variation of the pressure coefficient with speeds is given by $P_o/\sqrt{1-M^2}$ (reference 5). Reference 6 and the results of tests in the 8-foot high-speed wind tunnel and in other tunnels show that, for airfoils, the theory may underestimate the effect of speed; the most probable cause of the discrepancy is the assumption made in the development of the theory that the induced velocities are negligibly small. It has sometimes been assumed that the variation of the pressure coefficient given by $P_o/\sqrt{1-M^2}$ applies to three-dimensional as well as to two-dimensional flow.

Figures 12 to 16 indicate that, where the value of the pressure coefficient P was less than -0.2 at low speed, the coefficient decreased (i.e., became more negative) as the speed was increased. At points where the value of P was between -0.1 and -0.2 at low speed, the coefficient remained virtually constant as the speed was increased; and, at points where the value of P was greater than -0.1 at low speed, the coefficient increased as the speed was increased. This apparent dependence of the type of pressure-coefficient variation on the magnitude of P may be a coincidence. The type of variation may depend on the proximity of the wing and may result from wing and fuselage pressures following different rates of variation. There is need for further investigation of the way in which pressures vary with speed. At points where the value of P was greater than -0.1 at low speeds, the effect of compressibility on the pressure coefficients

was opposite from that expected on the basis of two-dimensional theory. The results show that, at high speeds, the magnitude of the pressure coefficients as predicted from pressure coefficients determined experimentally at low speed by application of the theoretical factor $1/\sqrt{1-M^2}$ may misrepresent the actual conditions.

At the points on the fuselage where the maximum negative pressures occurred, the effect of compressibility on the pressure coefficients agreed fairly well with the variation given by the two-dimensional theory, as is shown in figure 17. The broken curve represents the theoretical value of P given by $P_o/\sqrt{1-M^2}$. The agreement is quite satisfactory up to $M \cong 0.6$ and indicates that the use of this theoretical factor to calculated maximum loads due to negative pressures, although usually not conservative, may be permissible. This agreement also indicates that it may be possible to use the maximum negative pressure coefficients obtained from low-speed tests to predict approximately the critical speed of the fuselage. This conclusion should be considered tentative until investigated by tests of other models.

Although these tests were made primarily to determine the air loads on the fuselage, it is interesting to note the effect of wing-fuselage interference on the critical speed of an airplane. A comparison of the pressure distribution for the fuselage alone with the pressure distribution for the fuselage and the wing combined (fig. 9) indicates that the critical speed of the fuselage in the presence of the wing will be lower than that of the fuselage alone (about 130 miles per hour at 59° F., lower for this wing-fuselage combination). The interference of the fuselage will act similarly to decrease the critical speed of the wing and, since the critical speed of the wing alone is generally lower than the critical speed of the fuselage alone, the wing of an airplane will generally have a critical speed lower than the critical speed of the fuselage.

CONCLUDING REMARKS

1. The highest negative pressures on the fuselage occurred near the wing and were more dependent on the wing than on the fuselage.

2. The results indicate that the critical speed of

the fuselage will be decreased because of the velocities induced by the wing. The fuselage interference will likewise increase the local velocities on the wing and thereby decrease the critical speed of the wing. Inasmuch as the local velocities on the wing are usually higher than the local velocities on the fuselage, the effect on the wing will be more critical.

3. At high speeds, the magnitude of the pressure coefficients as predicted by the application of the theoretical factor $1/\sqrt{1-M^2}$ (where M is the ratio of the air speed to the speed of sound in air) to pressure coefficients measured at low speeds may misrepresent the actual conditions. At the points where the maximum negative pressures occurred, however, the variation of the pressure coefficient with speed was in good agreement with the factor $1/\sqrt{1-M^2}$, at least up to M = 0.58 (440 miles per hour at 59° F.), and may give satisfactory predictions of critical speed from data obtained at low speeds.

Langley Memorial Aeronautical Laboratory,
National Advisory Committee for Aeronautics,
Langley Field, Va., September 11, 1939.

REFERENCES

1. Rogallo, Francis M., and Gauvain, William E.: Wind-Tunnel Investigation of Air Inlet and Outlet Openings for Aircraft. N.A.C.A. confidential report, 1938.

2. Robinson, Russell G.: Sphere Tests in the N.A.C.A. 8-Foot High-Speed Tunnel. Jour. Aero. Sci., vol. 4, no. 5, March 1937, pp. 199-201.

3. Abbott, Ira H.: Fuselage-Drag Tests in the Variable-Density Wind Tunnel: Streamline Bodies of Revolution, Fineness Ratio of 5. T.N. No. 614, N.A.C.A., 1937.

4. Freeman, Hugh B.: Pressure-Distribution Measurements on the Hull and Fins of a 1/40-Scale Model of the U.S. Airship "Akron." T.R. No. 443, N.A.C.A., 1932.

5. Ackeret, J.: Über Luftkräfte bei sehr grossen Geschwindigkeiten insbesondere bei ebenen Strömungen. Helvetica Physica Acta, vol. I, fasc. 4, 1928, pp. 301-322.

6. Stack, John, Lindsey, W. F., and Littell, Robert E.: The Compressbility Burble and the Effect of Compressibility on Pressures and Forces Acting on an Airfoil. T.R. No. 646, N.A.C.A., 1938.

Figure 1a.- Front view. Model used in test.

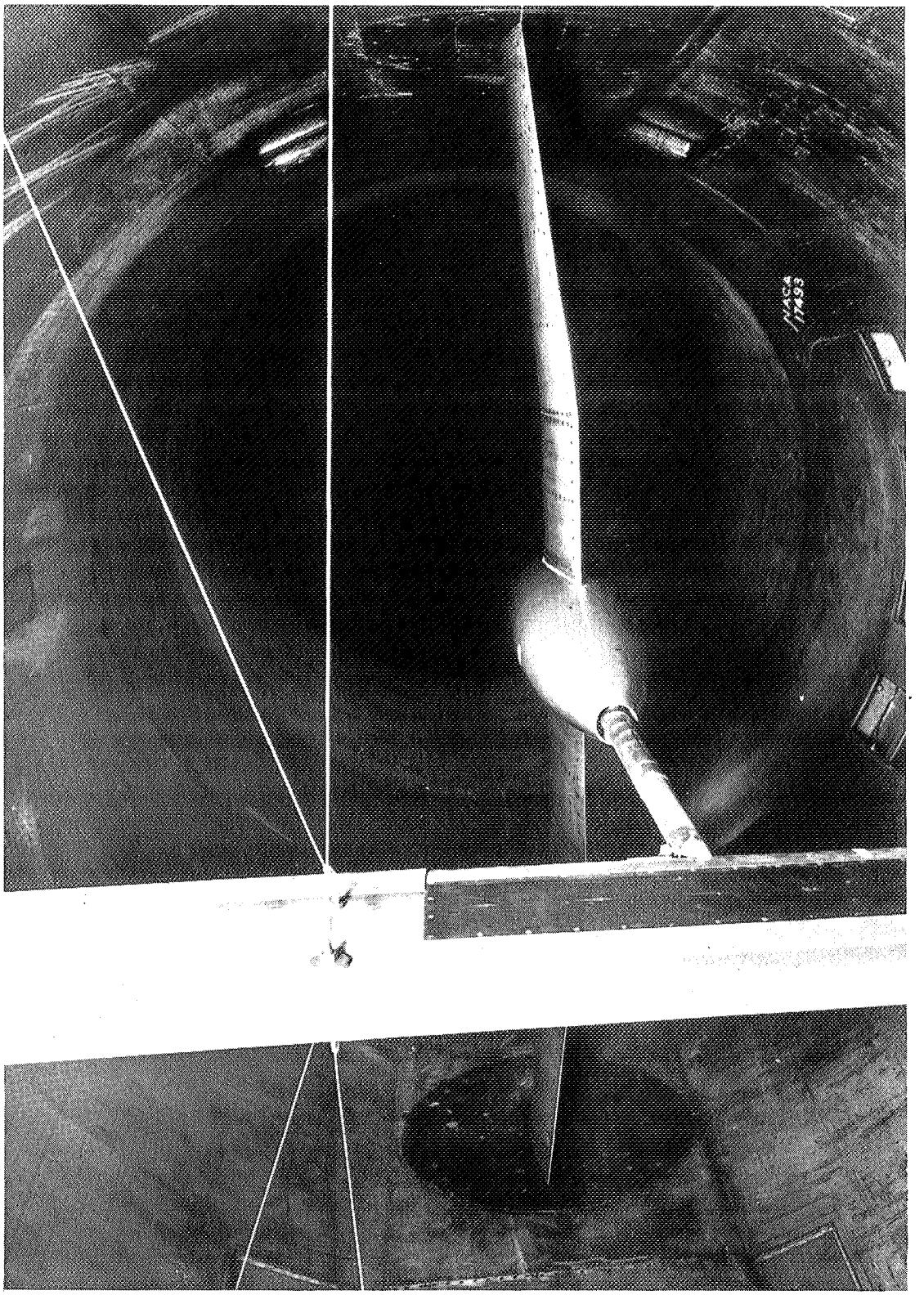

Figure 1b.- Rear view. Model used in test.

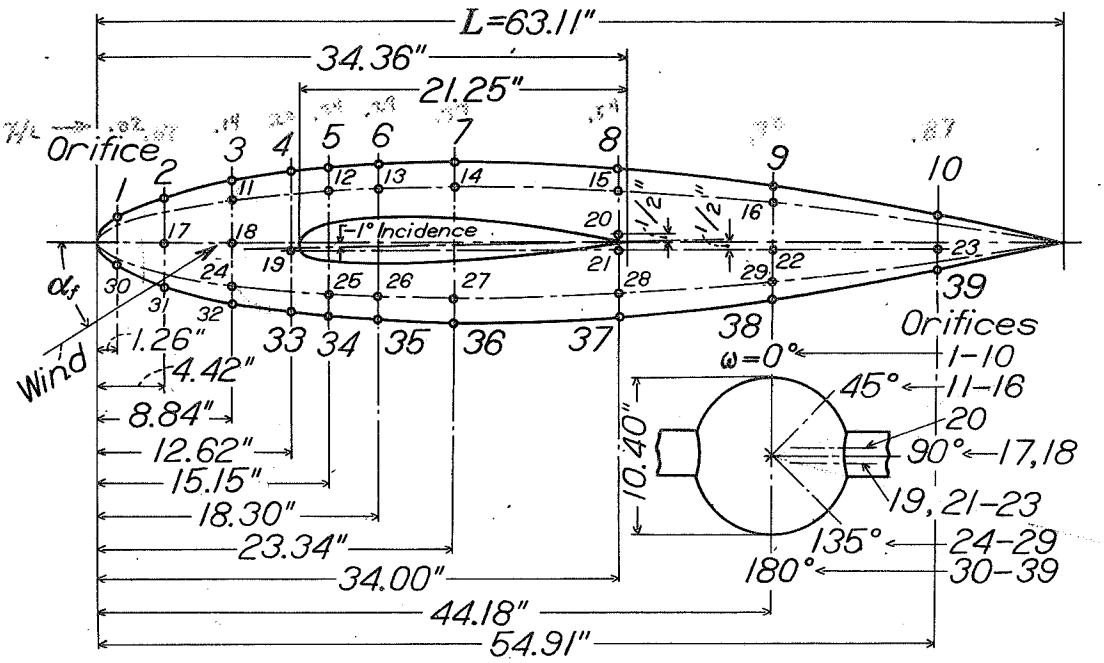

Figure 2.- Location of pressure orifices on the fuselage.

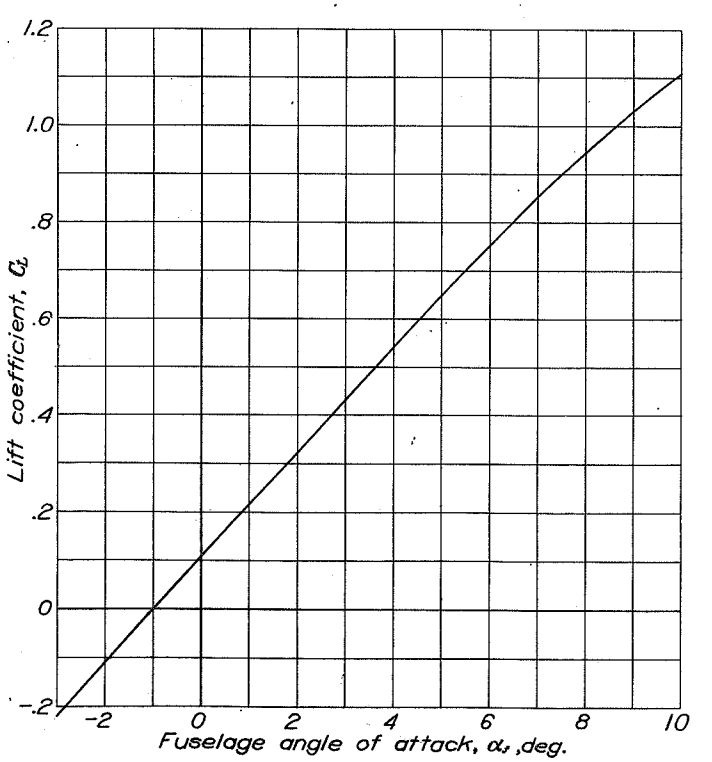

Figure 3.- Variation of lift coefficient with angle of attack for the wing-fuselage combination tested. M, 0.182; R, 1,760,000.

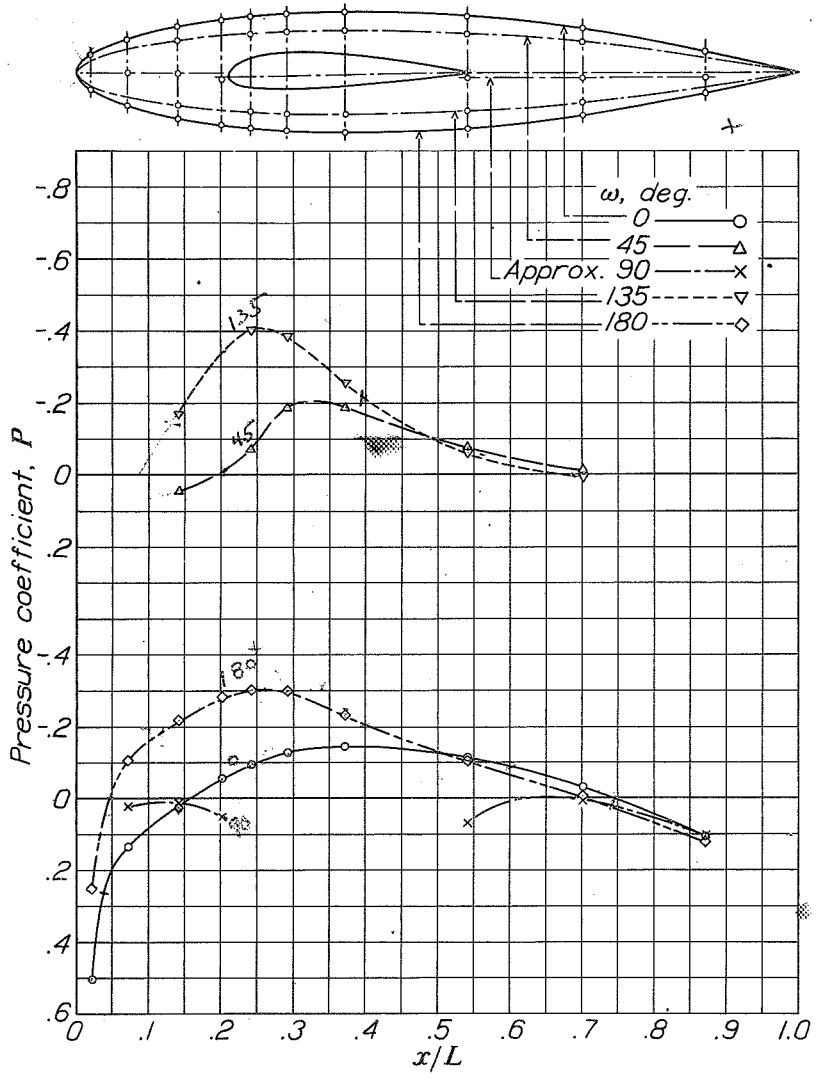

Figure 4.- Pressure distribution on fuselage. α_f, -3°; M, 0.182.

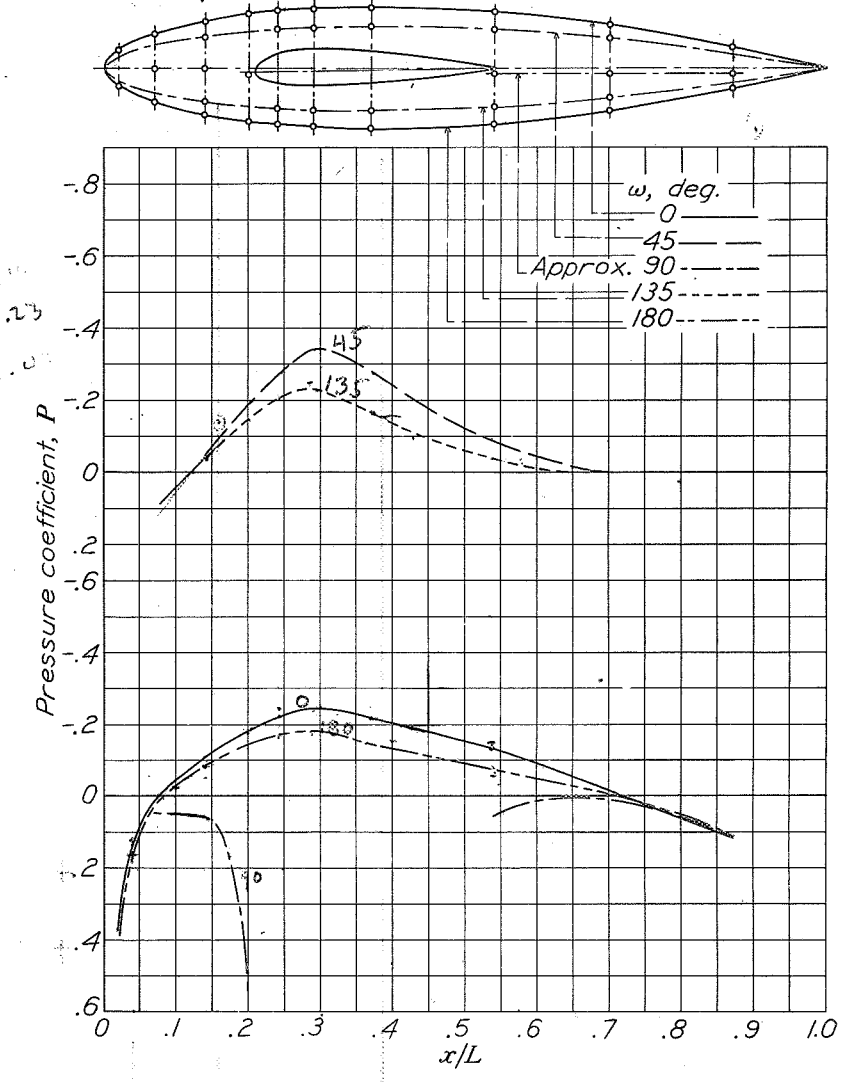

Figure 5.- Pressure distribution on fuselage. α_f, 0°; M, 0.182.

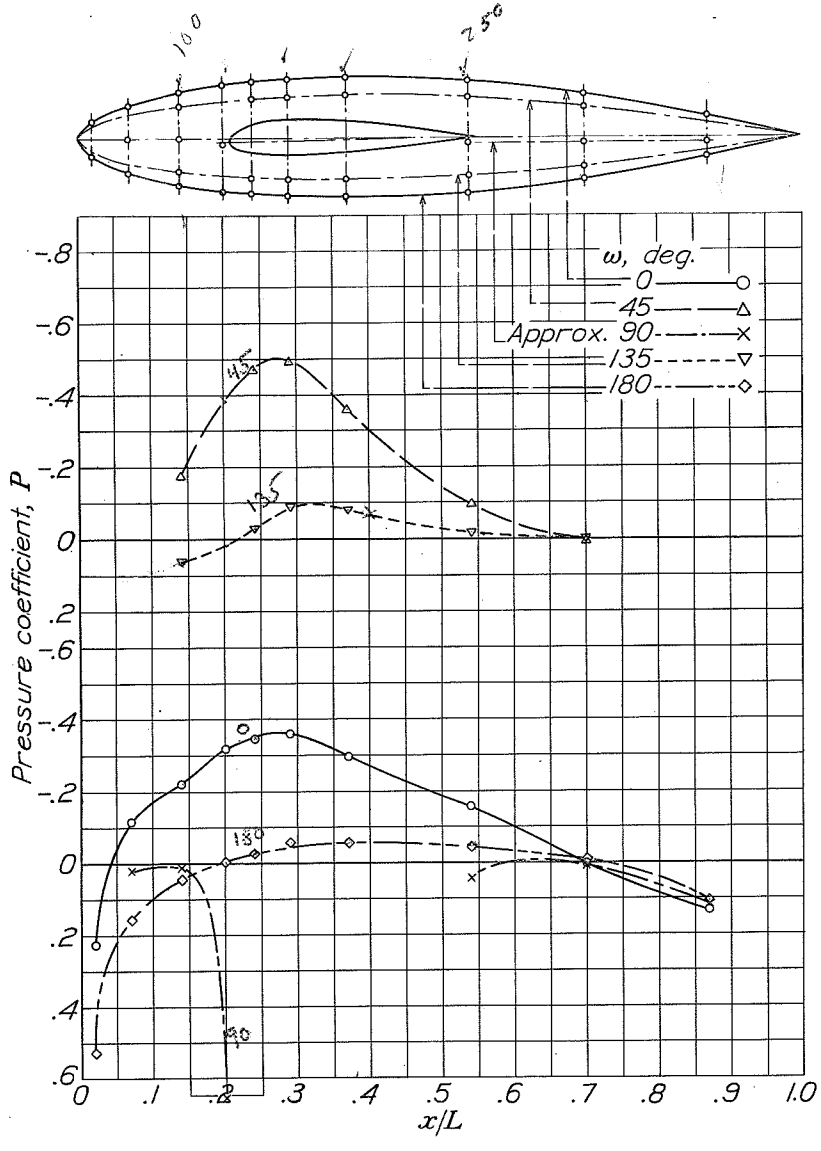

Figure 6.- Pressure distribution on fuselage. α_f, 3°; M, 0.182.

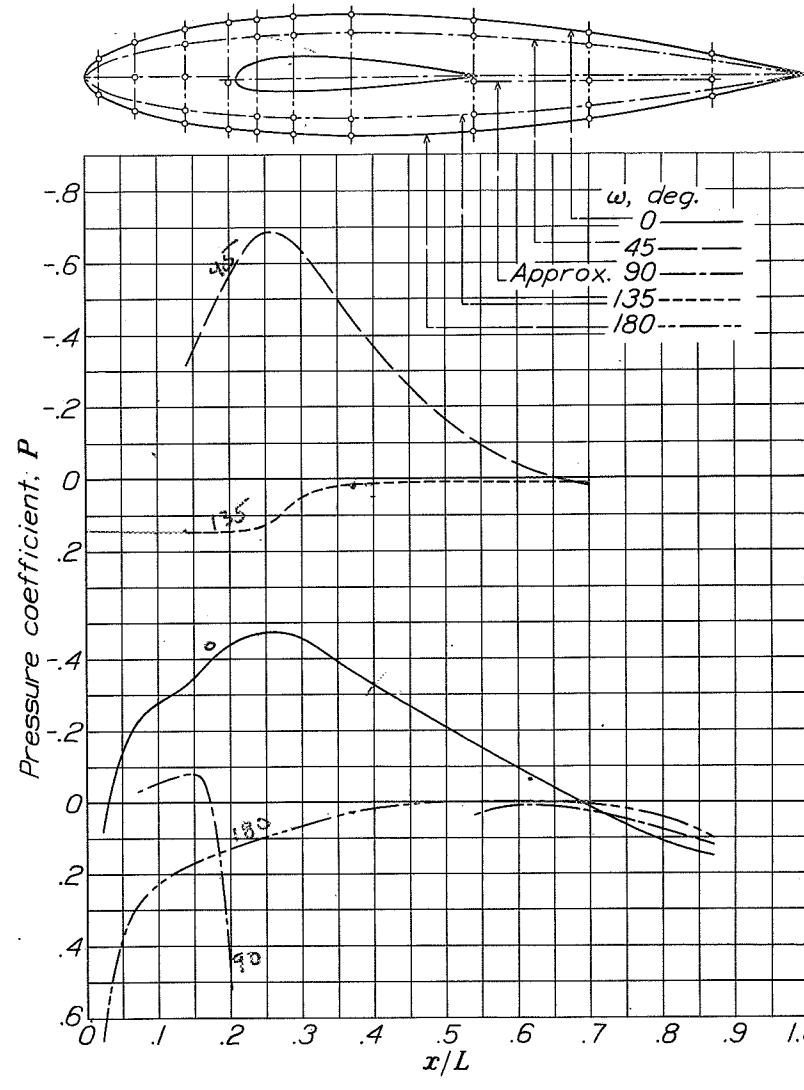

Figure 7.- Pressure distribution on fuselage. α_f, 6°; M, 0.182.

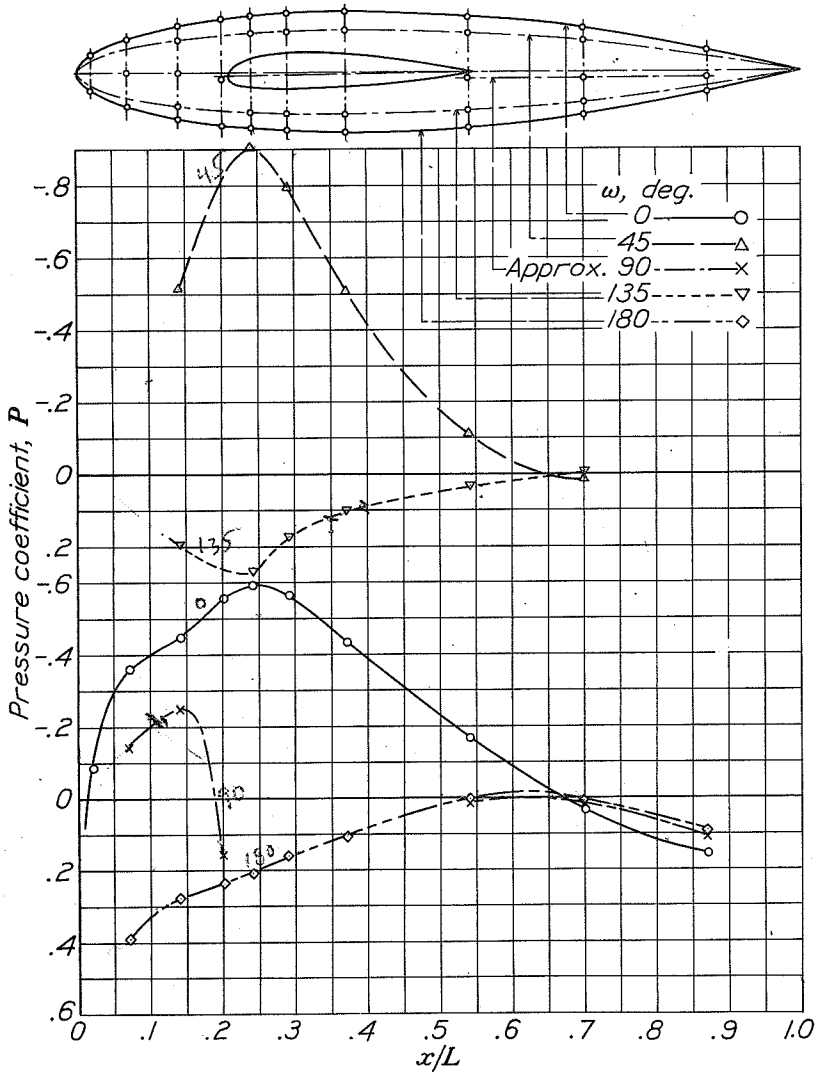

Figure 8.- Pressure distribution on fuselage. α_f, 9°; M, 0.182.

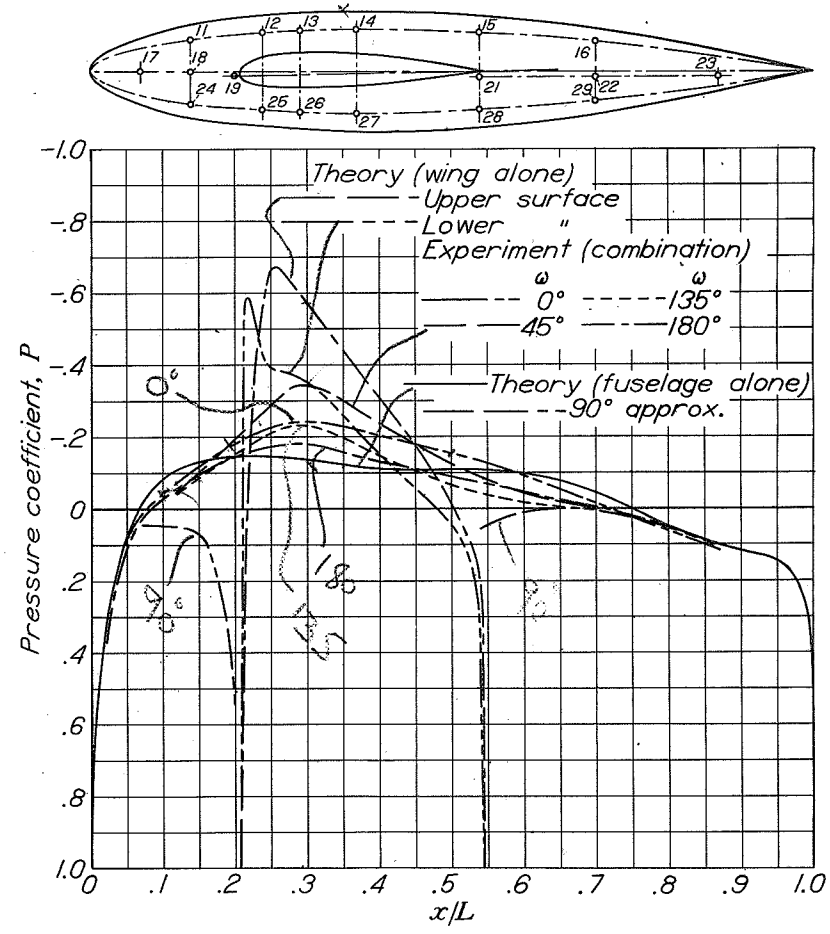

Figure 9.- Comparison of theoretical pressures on the wing alone and on the fuselage alone with the experimental pressures of the combination. α_f, 0°; M, 0.182.

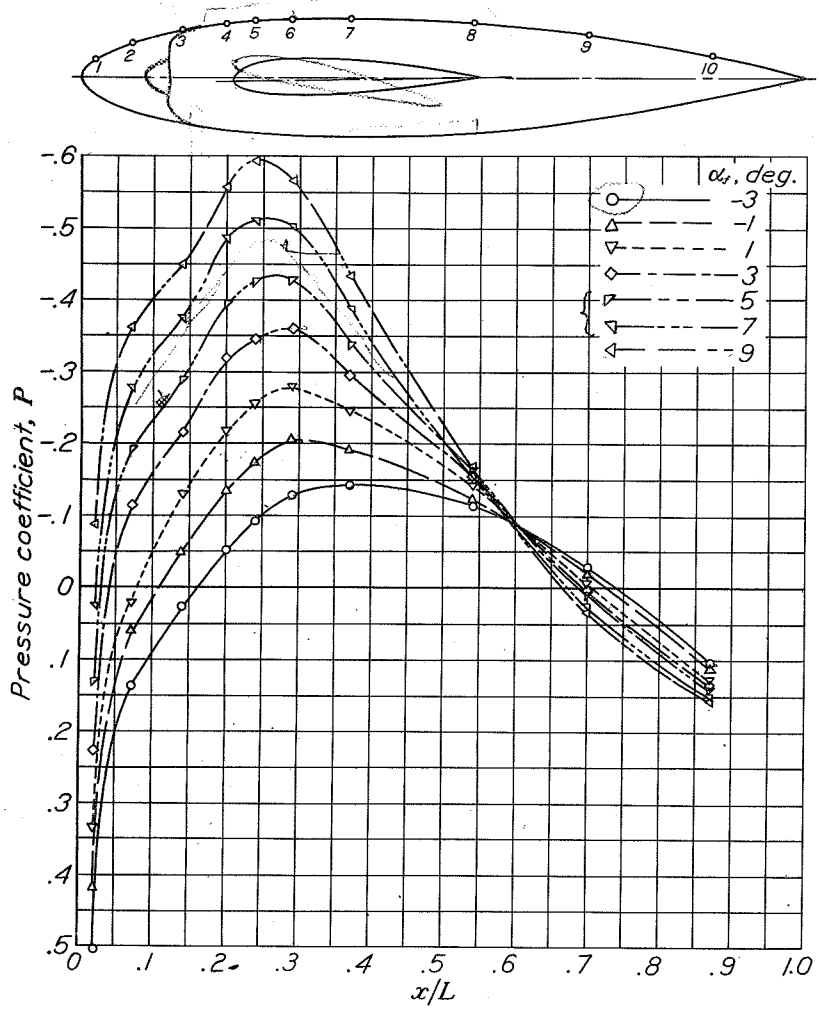

Figure 10.- Pressure distribution on fuselage. ω, 0°; M, 0.182.

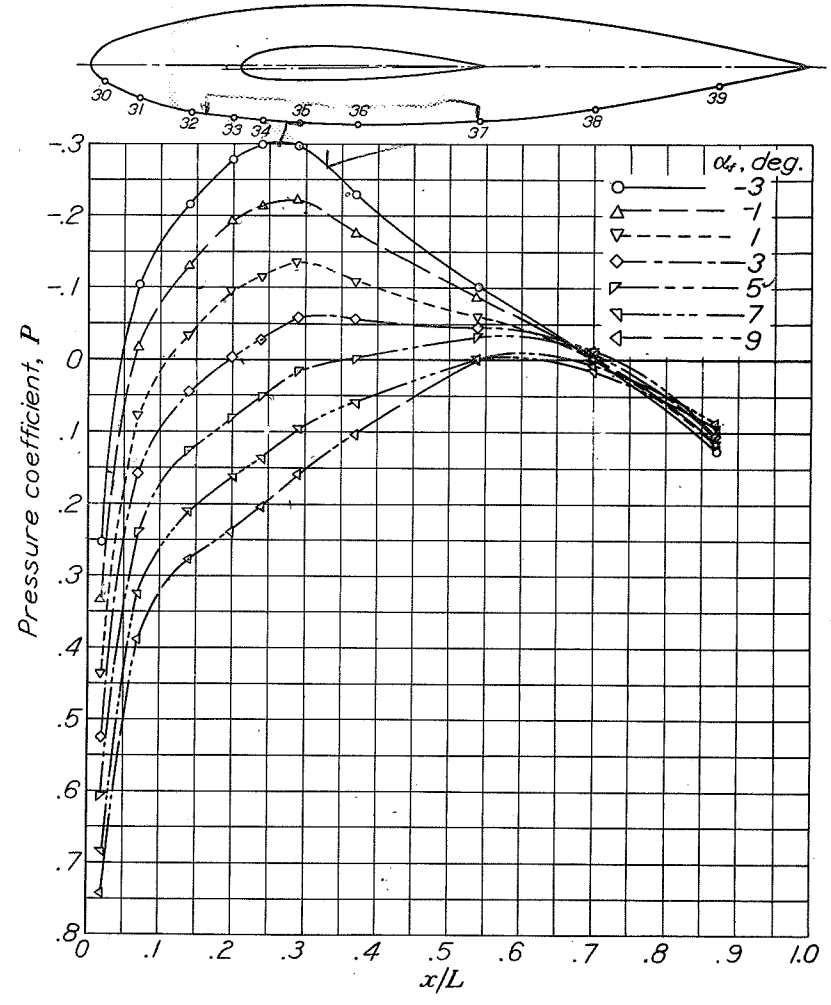

Figure 11.- Pressure distribution on fuselage. ω, 180°; M, 0.182.

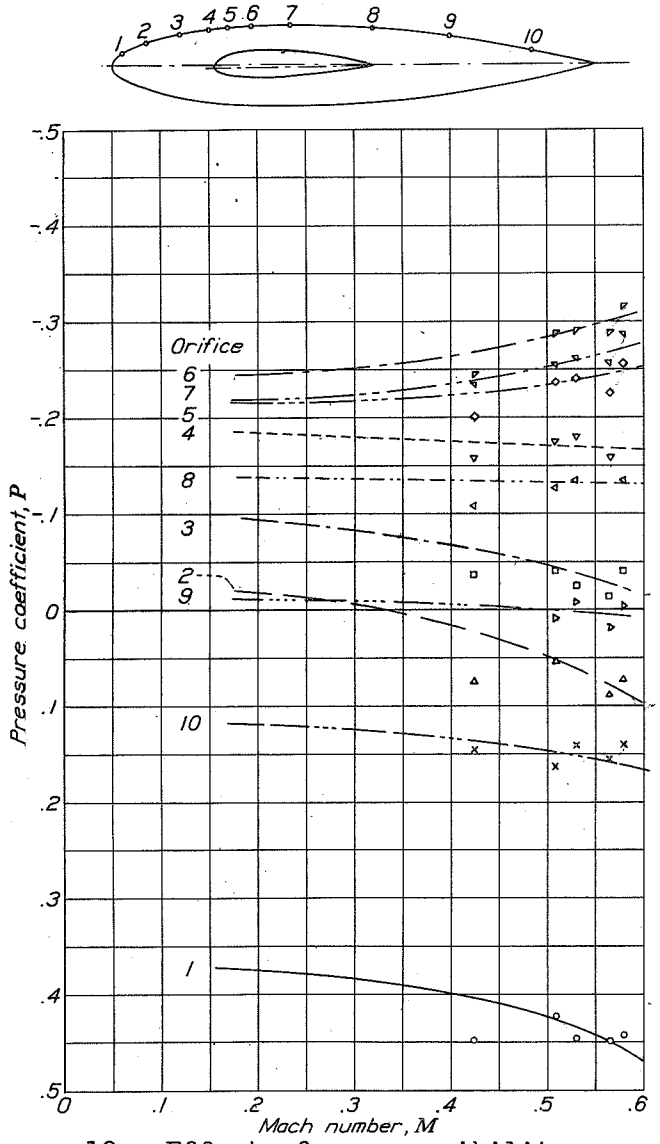

Figure 12.- Effect of compressibility on pressures. α_f, 0°; ω, 0°.

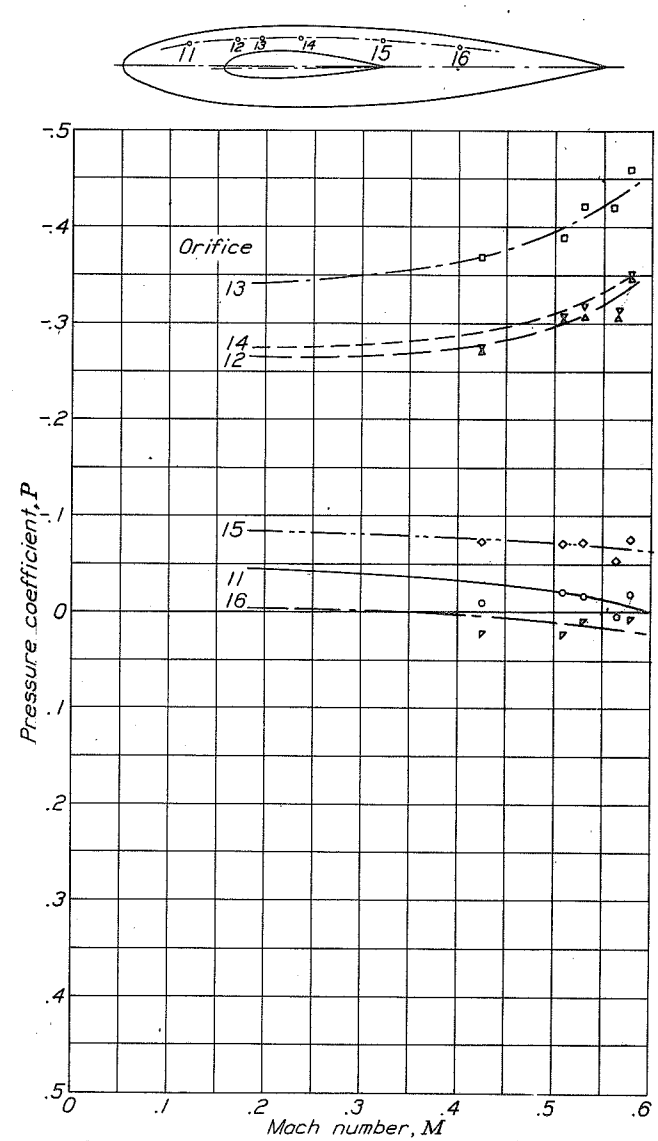

Figure 13.- Effect of compressibility on pressures. α_f, 0°; ω, 45°.

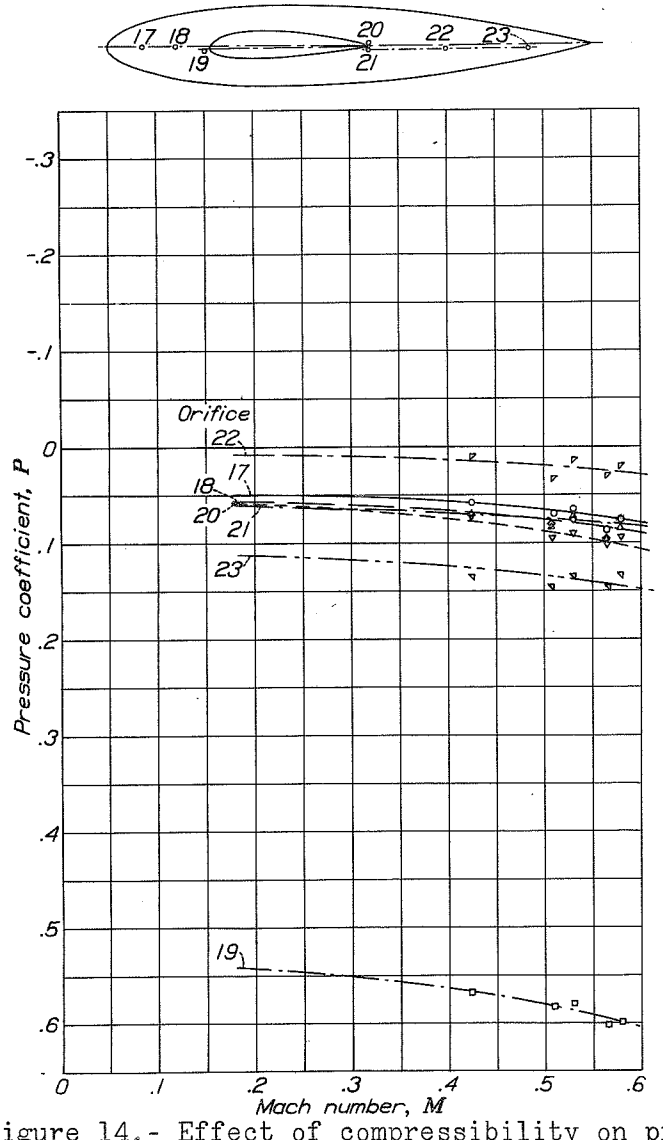

Figure 14.- Effect of compressibility on pressure. α_f, 0°; ω, approximately 90°.

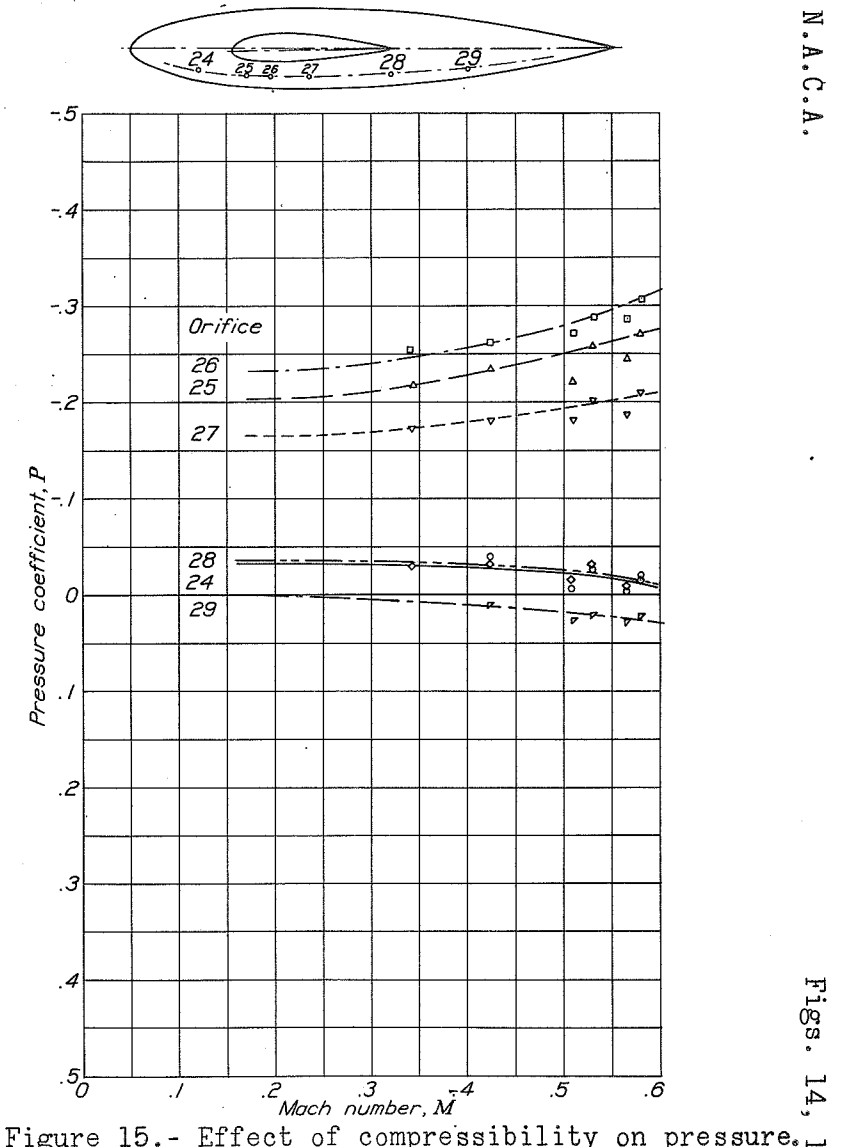

Figure 15.- Effect of compressibility on pressure. α_f, 0°; ω, 135°.

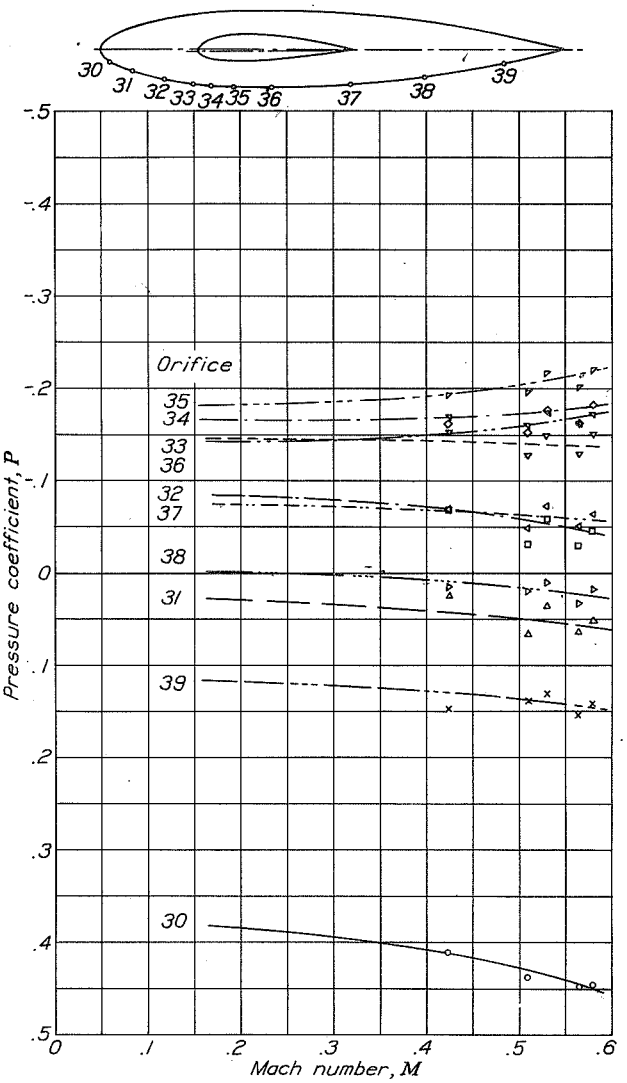

Figure 16.- Effect of compressibility on pressure.
α_f, 0°; ω, 180°.

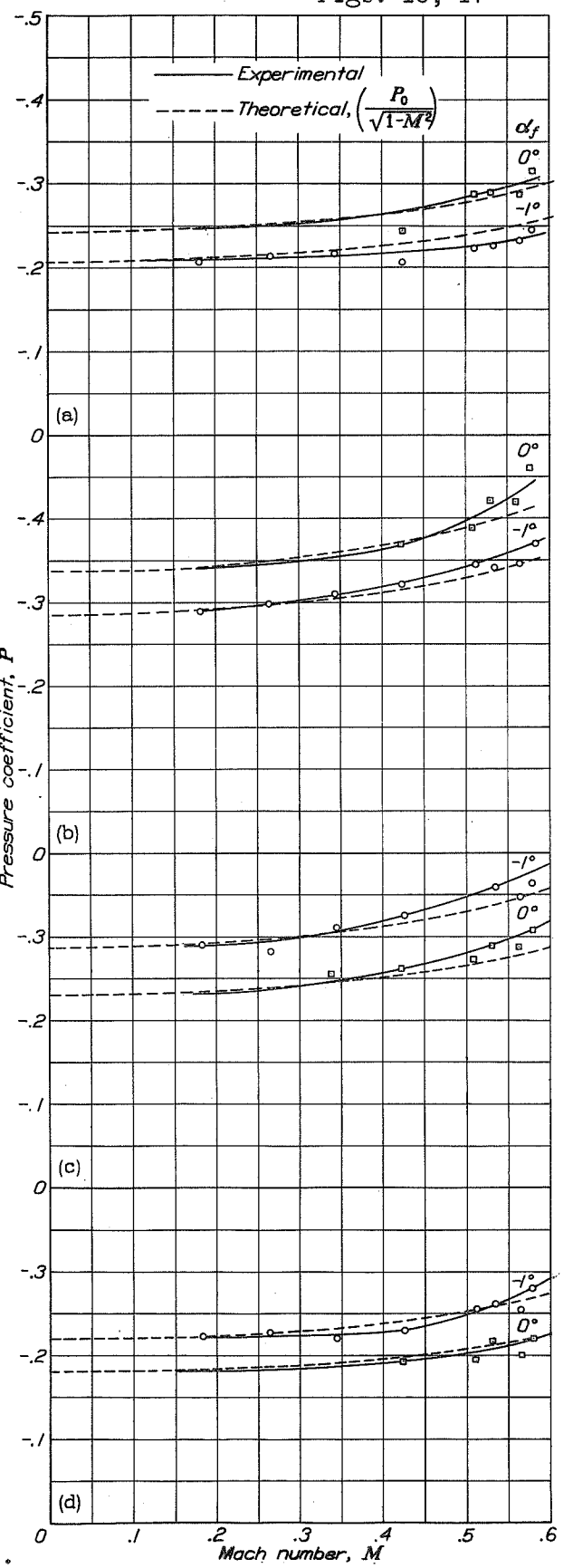

(a) Orifice 6. (b) Orifice 13.
(c) Orifice 26. (d) Orifice 35.
Figure 17.- Comparison of theoretical and experimental pressures.